OPEN ACCESS Freely available online

PLoS GENETICS

Quaking Regulates *Hnrnpa1* Expression through Its 3′ UTR in Oligodendrocyte Precursor Cells

N. Ruth Zearfoss, Carina C. Clingman, Brian M. Farley, Lisa M. McCoig†, Sean P. Ryder*

Department of Biochemistry and Molecular Pharmacology, University of Massachusetts Medical School, Worcester, Massachusetts, United States of America

Abstract

In mice, Quaking (*Qk*) is required for myelin formation; in humans, it has been associated with psychiatric disease. QK regulates the stability, subcellular localization, and alternative splicing of several myelin-related transcripts, yet little is known about how QK governs these activities. Here, we show that QK enhances *Hnrnpa1* mRNA stability by binding a conserved 3′ UTR sequence with high affinity and specificity. A single nucleotide mutation in the binding site eliminates QK-dependent regulation, as does reduction of QK by RNAi. Analysis of exon expression across the transcriptome reveals that QK and hnRNP A1 regulate an overlapping subset of transcripts. Thus, a simple interpretation is that QK regulates a large set of oligodendrocyte precursor genes indirectly by increasing the intracellular concentration of hnRNP A1. Together, the data show that hnRNP A1 is an important QK target that contributes to its control of myelin gene expression.

Citation: Zearfoss NR, Clingman CC, Farley BM, McCoig LM, Ryder SP (2011) Quaking Regulates *Hnrnpa1* Expression through Its 3′ UTR in Oligodendrocyte Precursor Cells. PLoS Genet 7(1): e1001269. doi:10.1371/journal.pgen.1001269

Editor: Harry T. Orr, University of Minnesota, United States of America

Received June 18, 2010; **Accepted** December 6, 2010; **Published** January 6, 2011

Funding: This work was supported by pilot award PP1418 from the National Multiple Sclerosis Society, a Worcester Foundation for Biomedical Sciences Scholar Award and by NIH Grant GM081422. The funders had no role in study design, data collection and analysis, decision to publish, or preparation of the manuscript.

Competing Interests: The authors have declared that no competing interests exist.

* E-mail: Sean.Ryder@umassmed.edu

†Deceased.

Introduction

Myelin is a lipid-rich structure that facilitates the propagation of electrical impulses along neuronal axons and protects them from degeneration [1–3]. In the central nervous system (CNS), myelin is produced by oligodendrocytes, glial cells that ensheathe nearby axons with specialized cytoplasmic processes. Defects in the formation and maintenance of myelin cause several devastating diseases in humans, including multiple sclerosis, leukodystrophy, and Pelizaeus-Merzbacher disease.

In the mouse, myelin formation requires QK, a STAR domain RNA-binding protein that regulates gene expression after transcription [4]. The *quaking viable* (Qk^{qk}) mutation, which causes a pronounced tremor, was discovered over forty years ago [5]. The phenotype is caused by the failure to form compact myelin in the CNS and derives from a large deletion lying upstream of the Quaking (*Qk*) locus [6]. The Qk^{qk} mutation eliminates oligodendrocyte expression of two cytoplasmic QK splice isoforms, QK-6 and QK-7, and reduces expression of a third nuclear isoform, QK-5, primarily in the more severely affected rostral areas [7]. In Qk^{qk} mice, expression of QK-6 under the control of the oligodendrocyte-specific proteolipid protein gene (*Plp1*) promoter rescues the myelin defect, demonstrating that QK-6 alone suffices to restore QK function [8]. Other alleles of *Qk* are embryonic lethal, except for the Qk^{e5} allele identified by Justice and coworkers that also causes severe demyelination [9].

QK is a multifunctional protein proposed to control myelin formation through three different mechanisms. First, QK stabilizes the myelin basic protein (*Mbp*), microtubule associated protein 1B (*Map1b*), and $p27^{Kip1}$ mRNAs in the brain or in cultured oligodendrocytes [10–12]. Second, QK controls the subcellular distribution of *Mbp* mRNA, such that an increase in the ratio of nuclear to cytoplasmic QK isoforms drives nuclear retention of *Mbp* mRNA and reduces *Mbp* translation [13]. Finally, QK regulates alternative splicing of *Mbp*, *Plp1*, and myelin associated glycoprotein (*Mag*) mRNAs [14]. Qk^{qk} mutant brains display altered isoform ratios of *Mbp*, *Plp1*, and *Mag* transcripts, and splicing of a *Mag* mini-gene is altered in the presence of exogenous QK-5 in cultured COS-7 cells [14]. How QK controls such diverse processes is unclear.

Quaking has recently been implicated in several human psychiatric diseases. Human Quaking (*QKI*) has been proposed to be a candidate gene for schizophrenia (SCZ). Genetic linkage analysis has identified a 0.5 Mb haplotype in the region of *QKI* that segregates with SCZ in a large Swedish pedigree [15]. Moreover, SCZ brains have a number of similarities with the brains of Qk^{qk} mice, including downregulation of *QKI* and a number of other myelin-related genes, including *MBP*, *MAG*, and *PLP11* [16–18]. Additionally, like Qk^{qk} brains, SCZ brains contain a number of mRNAs that are present at abnormal splice isoform ratios [19–22]. Some of these, including *Mag*, are also mis-spliced in the Qk^{qk} mouse, suggesting that splicing alterations in the Qk^{qk} mouse and in SCZ brains could share a common mechanism [16]. Other clinical phenotypes in which disruptions in QK function are thought to contribute to disease include major depressive disorder and 6q terminal deletion syndrome [23,24].

Despite the importance of QK for myelination and its implications for human health, relatively few direct targets have been identified. Thermodynamic binding analysis and SELEX have shown that the sequence element ACUAAY, alternatively termed the Quaking Star Binding Element (QSBE) or Quaking Response Element (QRE), is required for a high affinity

Author Summary

Myelin is a lipid-rich structure that insulates neuronal axons, facilitating electrical conductance and protecting neurons from degeneration. Myelin comprises multiple compact layers of phospholipid bilayer and specific myelin proteins that occupy distinct positions within the structure. In the central nervous system, an RNA–binding protein termed Quaking is required for formation of compact myelin. Quaking regulates the production of several myelin-related proteins by binding to their mRNAs. Quaking controls the overall levels of these proteins and controls the relative amount of sequence variants of the proteins generated through alternative splicing. Here, we identify a new Quaking mRNA target, the *Hnrnpa1* transcript. We show that Quaking regulates the overall level of hnRNP A1. Because hnRNP A1 is itself an RNA regulatory factor and has been implicated in the control of alternative splicing, regulation of hnRNP A1 by Quaking may have consequences for the expression of multiple additional targets. We show that hnRNP A1 and Quaking regulate an overlapping set of transcripts and exons in myelin-forming cells of the central nervous system.

interaction between purified QK protein and its target RNA [25,26]. Additionally, a recent cross-link immunoprecipitation study using chemically modified nucleotides detected binding to the sequence ACUAAY and an additional sequence variant AUUAAY [27]. It remains unclear how binding affinity *in vitro* correlates to binding site occupancy and regulation *in vivo*. The relative simplicity of the binding determinant, which is predicted to occur approximately once per kb of random RNA sequence, suggests that the binding element may not be sufficient to specify mRNA targets [28]. A single QSBE is present within the 3′UTR of *Mbp* mRNA in a region required for post-transcriptional regulation of *Mbp* expression [25,26]. However, a region of *Mag* pre-mRNA that has been shown experimentally to drive QK-dependent splicing events does not contain a QSBE or the variant AUUAAY [14]. Here, we set out to determine whether the QK binding element mediates QK-dependent regulation in *Mbp* and other regulatory targets. We show that QK regulation of *Mbp* expression requires the QSBE. Additionally, we identify a novel target, *Hnrnpa1* mRNA, and show that QK regulates *Hnrnpa1* expression in a similar fashion to *Mbp*. Finally, we show that hnRNP A1 contributes to QK control of myelin gene expression in genome wide analyses.

Results

The QSBE is a functional regulatory element within the *Mbp* 3′ UTR

It has previously been shown that QK interacts with a region of the *Mbp* 3′ UTR and that the core element required for the interaction is the sequence ACUAAY [25,26]. SELEX experiments suggest that a nearby YAAY may also contribute to target selection [26]. We asked whether the QSBE is required for post-transcriptional regulation of mRNA by QK.

To test whether the QSBE is a required element within the *Mbp* 3′ UTR, we established a quantitative two-color fluorescence reporter assay in CG-4 oligodendrocyte precursor cells, an immortalized cell line (Figure 1A, Figure S1A, S1B, S1C) [29]. CG-4 cells can be maintained in culture as progenitors or induced to differentiate into mature oligodendrocytes, can be transfected, and express QK and a relevant QK target population. Additionally, their use avoids the potential complications of the Qk^{qk} mouse, in which the genetic lesion lies upstream of the *Qk* locus and deletes parts of two additional genes [6,30]. A complete *Qk* knockout is embryonic lethal [31].

We compared expression of a GFP reporter bearing the *Mbp* 3′ UTR to a reporter bearing a mutant *Mbp* 3′ UTR harboring a U to G point mutation that blocks binding of QK to the RNA (Figure 1B) [25]. All other aspects of the constructs were identical. We observed three-fold less reporter mRNA in cells transfected with the mutant construct compared to the wild type (relative expression 0.36 ± 0.07, $p=0.02$) (Figure 1C). In contrast, GFP reporter fluorescence increased by a small amount as a result of the mutation (relative expression 1.38 ± 0.20, $p=0.04$) (Figure 1C). Dividing the protein expression by the mRNA expression gives a representation of the efficiency of mRNA translation [32]. The QSBE mutant yields four-fold more reporter protein per unit RNA compared to the wild-type reporter (relative value 3.83 ± 0.93, $p=0.03$) (Figure 1C). In total, we observed two opposing effects of the QSBE in the *Mbp* 3′ UTR: a positive effect on mRNA level and a negative effect on the efficiency of translation. These results demonstrate that the QSBE is a functional *cis*-regulatory element within the *Mbp* 3′ UTR and are consistent with published findings that QK positively controls *Mbp* mRNA stability and negatively controls its translation through nuclear retention of its mRNA [10,13].

QK interacts with a QSBE within the 3′ UTR of the *Hnrnpa1* mRNA

In addition to promoting mRNA stability, QK regulates alternative splicing. However, the sequence that has been experimentally shown to drive QK dependent splicing, the *Mag* splicing control element, does not contain the QSBE sequence or the variant AUUAAY [14]. Moreover, recombinant QK does not interact with the *Mag* splicing control sequence or the splicing control sequence of another QK target, *Plp1*, by electromobility shift assays [33,34] (Figure S2). The site of QK binding could lie distal to the minimal QK-responsive splicing elements that have been described. Alternatively, accessory proteins found in the nucleus might modify QK binding specificity, bringing it to other targets. A third and simpler possibility is that the effect of QK on alternative splicing could be a secondary consequence of deregulation of another factor.

To test the final hypothesis, we first determined the ability of QK to associate with five splicing factor mRNAs (*Hnrnpa1*, *Tra2b*, *Sfrs5*, *Prpf4b*, and *Slu7*) that contain a QSBE in their 3′ UTRs by RNA-immunoprecipitation from mouse brain lysate. We were unable to detect an interaction between QK and *Sfrs5*, *Tra2b*, *Prpf4b*, and *Slu7* mRNAs using an anti-QK antibody that recognizes all three QK isoforms (Figure S3). In contrast, we observe association of QK with *Hnrnpa1* mRNA, which contains a single QSBE sequence within a conserved region of its 3′ UTR (Figure 2A), in both uncrosslinked and formaldehyde crosslinked brain lysates (Figure 2B, 2C). In uncrosslinked brain lysates, QK antibodies immunopreciptate 20% of the input *Hnrnpa1* mRNA, and 3% of control *Sf3b1* mRNA, which encodes a core spliceosomal component. The formaldehyde crosslinking experiment controls for the possibility of QK repartioning during extract preparation, while the uncrosslinked experiment confirms that the crosslinking agent is not capturing a transient association.

To determine whether QK binds the QSBE within the *Hnrnpa1* 3′ UTR with high affinity and specificity, we used gel mobility shift and fluorescence polarization (FP) assays to measure the association of recombinant, purified QK RNA-binding domain with a 30 nucleotide synthetic RNA derived from the *Hnrnpa1* 3′

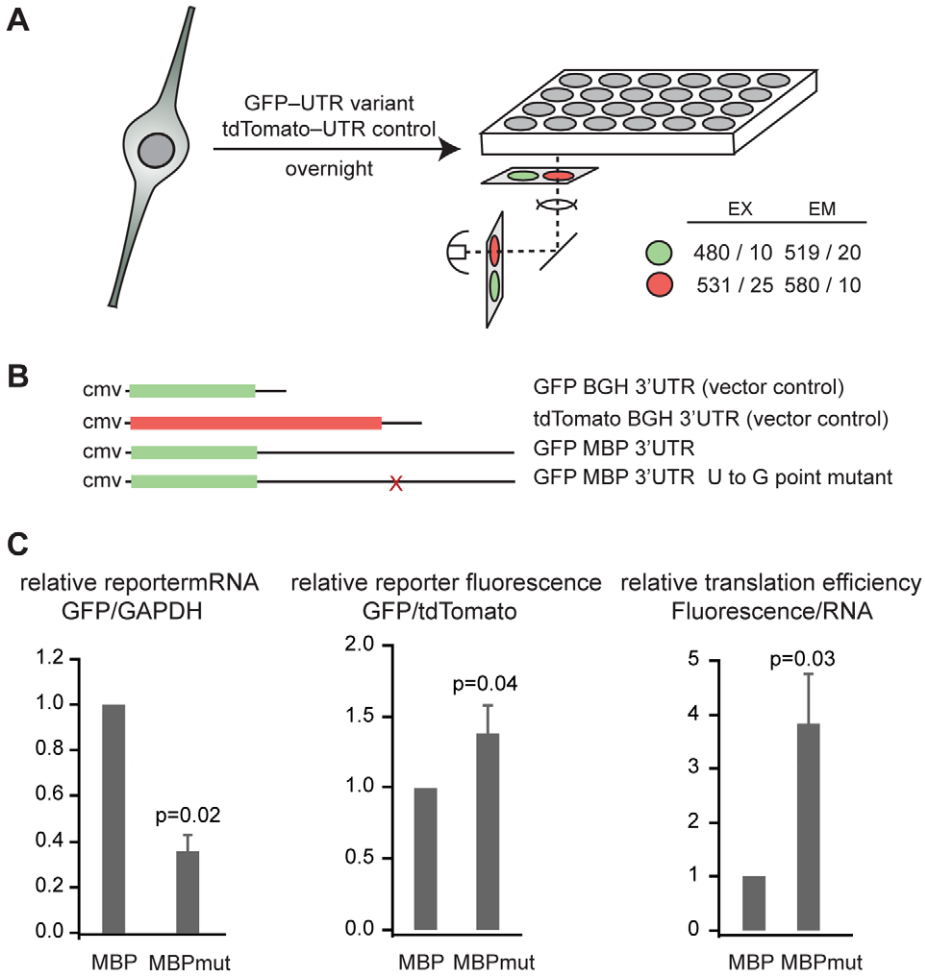

Figure 1. The QSBE is a regulatory element in the *Mbp* 3′ UTR. (A) Schematic drawing of the fluorescence reporter assay. (B) Constructs used in reporter assays. The *Mbp* 3′ UTR or the *Mbp* 3′ UTR with the U to G point mutation were inserted into the 3′ UTR of phrGFPII-1. tdTomato was unmodified and served as a transfection control. (C) tdTomato and GFP mRNA level were measured by real time RT-PCR from cells co-transfected with the indicated GFP construct and the tdTomato transfection control. The data in the graph are the average and standard deviation of six replicates from two independent experiments. The ratio of green to red fluorescence intensity was determined from nine replicates in three independent experiments. The graph represents the average and standard deviation. The normalized reporter fluorescence was divided by the normalized reporter mRNA to obtain a measure of translational efficiency. Error bars represent the error propagated from the standard deviation of the reporter fluorescence and real time RT-PCR data.
doi:10.1371/journal.pgen.1001269.g001

UTR and containing the QSBE (Figure 2A). The $K_{d,app}$ for binding was 36±2 nM; a U to G mutation within the QSBE reduced binding by >50-fold (Figure 2D, 2E). The previously identified *Mbp* QSBE bound with an apparent K_d of 44±2 nM, and the interaction was competed with a 12-nucleotide *Hnrnpa1* RNA containing the core ACUAAY motif (Figure 2E).

QK controls *Hnrnpa1* mRNA abundance and translational efficiency

We used the GFP reporter assay to test whether the QSBE from *Hnrnpa1* functions in cultured CG-4 cells (Figure 3A). The U to G point mutation within the *Hnrnpa1* 3′ UTR that eliminated QK binding in vitro (Figure 2D) reduced reporter mRNA level by approximately five-fold (relative expression 0.21±0.04, p = 0.001), consistent with a role for QK in promoting mRNA stability (Figure 3B). As with the *Mbp* reporter, the binding site mutation had a small increase on the amount of fluorescent protein produced (1.36±0.2, p = 0.001) (Figure 3C). The same increase was also observed using an independent dual luciferase reporter assay in which the *Hnrnpa1* 3′ UTR containing the wild-type or the U-to-G point mutant QSBE was inserted into the *Renilla reniformis* luciferase 3′ UTR (1.9±0.5, p = 0.02) (Figure 3D). *Renilla* expression also increased in a CG-4 cell line that stably expresses a *Qk* $shRNA^{miR}$ (1.53±0.05, p = 0.04)(Figure 3D). We were unable to test the effect of *Qk* $shRNA^{miR}$ in the GFP reporter assay because the $shRNA^{miR}$ construct also expresses GFP.

To obtain a measure of translational efficiency, we divided the normalized reporter fluorescence by the normalized amount of reporter mRNA [35]. Translational efficiency of the QSBE mutant *Hnrnpa1* 3′ UTR was increased (6.58±1.66, p = 0.014) compared to the construct without the mutation (Figure 3E), indicating that the QSBE mutation increases the efficiency of translation of the reporter transcript. We were not able to determine reporter mRNA concentration using the luciferase reporter assay because of persistent contaminating reporter DNA. Together the data establish that QK binds the *Hnrnpa1* 3′ UTR through the QSBE and that this binding enhances *Hnrnpa1* mRNA stability but reduces its translation. The results parallel the data collected using the *Mbp* reporter.

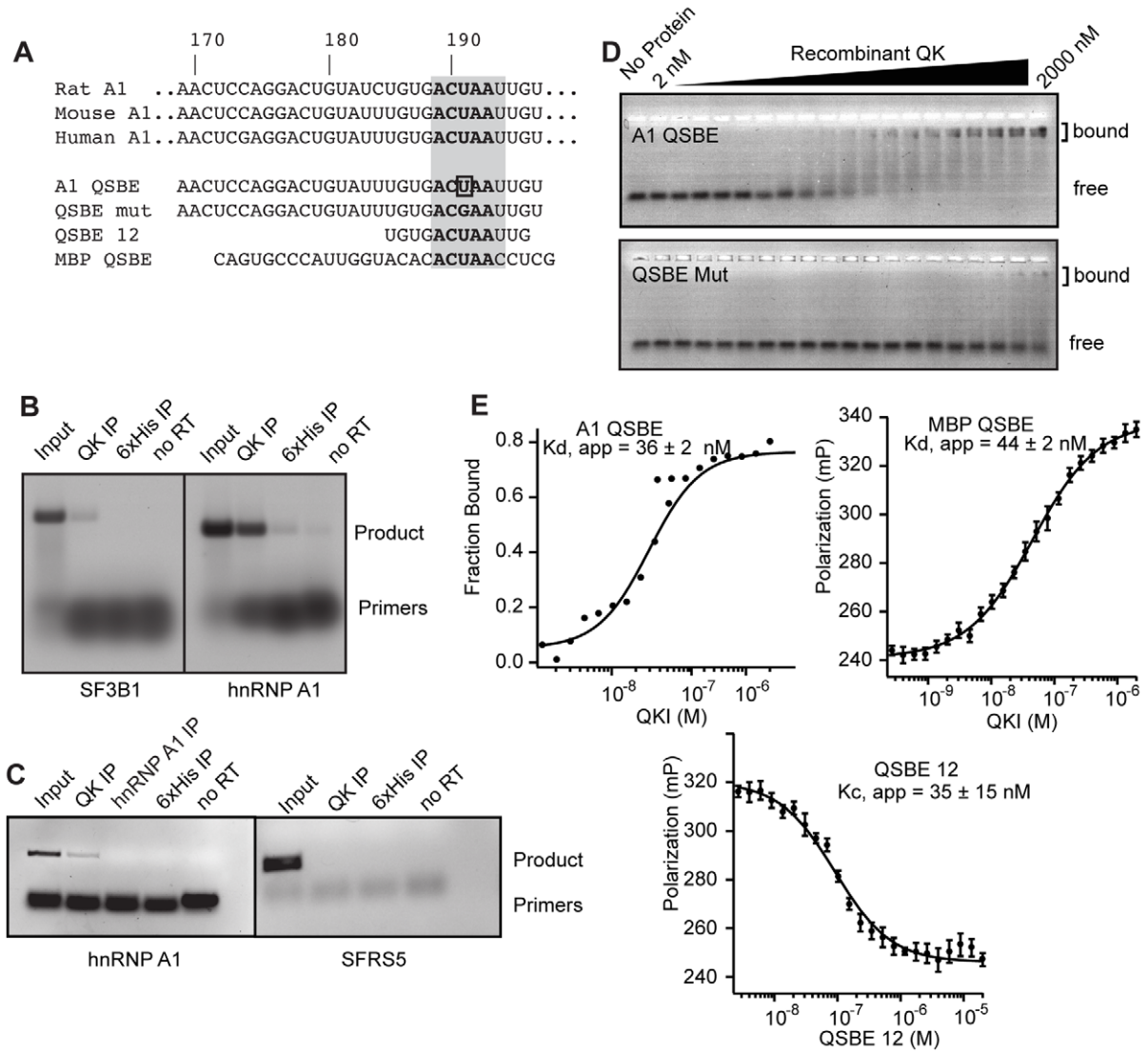

Figure 2. QK binds to an element in the *Hnrnpa1* 3′ UTR. (A) Mouse, rat, and human *Hnrnpa1* 3′ UTRs contain the ACUAA element in a conserved UTR region. Also included are the sequences analyzed by gel shift and fluorescence polarization assays, including the U to G point mutant, and the *Mbp* QSBE for comparison. (B) *Hnrnpa1* mRNA co-immunoprecipitated with QK from mouse brain lysate. Lanes are as indicated. (C) *Hnrnpa1* mRNA co-precipitated from a lysate prepared from formaldehyde crosslinked mouse brain tissue. Lanes are as indicated. Products were detected in an ethidium bromide stained gel. (D) Electrophoretic mobility shift assays demonstrate a high affinity interaction between QK and the wild type *Hnrnpa1* QSBE in vitro. The U to G point mutant, QSBE Mut, did not interact. (E) EMSA and fluorescence anisotropy assays demonstrating an interaction between QK and the *Mbp* QSBE of similar affinity and competition of the interaction with a 12 nucleotide *Hnrnpa1* 3′ UTR fragment containing ACUAA. Error bars indicate the standard deviation of five reads of each polarization measurement for each experiment. The error indicated for $K_{d,\ app}$ and $K_{c,\ app}$ is the standard deviation of at least three experiments.
doi:10.1371/journal.pgen.1001269.g002

The reporter constructs isolate 3′-UTR dependent regulation of *Hnrnpa1*. However, *Hnrnpa1* expression is also regulated in 3′-UTR-independent ways. For example, hnRNP A1 is known to regulate its own alternative splicing [36]. Moreover, hnRNP A1 protein stability or indirect regulation of hnRNP A1 transcription would not factor into reporter expression measurements. It is therefore important to determine the overall effect of QK on the amount of endogenous hnRNP A1. We measured *Hnrnpa1* mRNA and protein levels in the *Qk* shRNA^{miR} knockdown CG-4 cell line compared to a non-targeting shRNA^{miR} line (Figure 4A) by qRT-PCR and Western blot. The *Qk* knockdown line exhibited a four-fold decrease in endogenous *Hnrnpa1* mRNA (0.25 ± 0.18, $p = 0.012$), which matches the effect of mutating the QSBE in the *Hnrnpa1* 3′-UTR reporter. We also observe a four-fold reduction in hnRNP A1 protein (0.24 ± 0.25, $P = 0.018$) in the *Qk* shRNA^{miR} line (Figure 4B, 4C), which contrasts with our 3′-UTR reporter data. Thus, we conclude that QK has a net positive effect on hnRNP A1 expression in CG-4 cells, and that QK-dependent regulation of *Hnrnpa1* mRNA stability is more important to endogenous hnRNP A1 expression than control of translation efficiency, at least in CG-4 oligodendrocyte precursors.

hnRNP A1 regulates *Mag* exon 12 alternative splicing

Because hnRNP A1 represses alternative splicing, misregulation of hnRNP A1 is predicted to alter splicing patterns in the Qk^{qk} mouse brain. Wu et al. [14] identified splicing changes in the

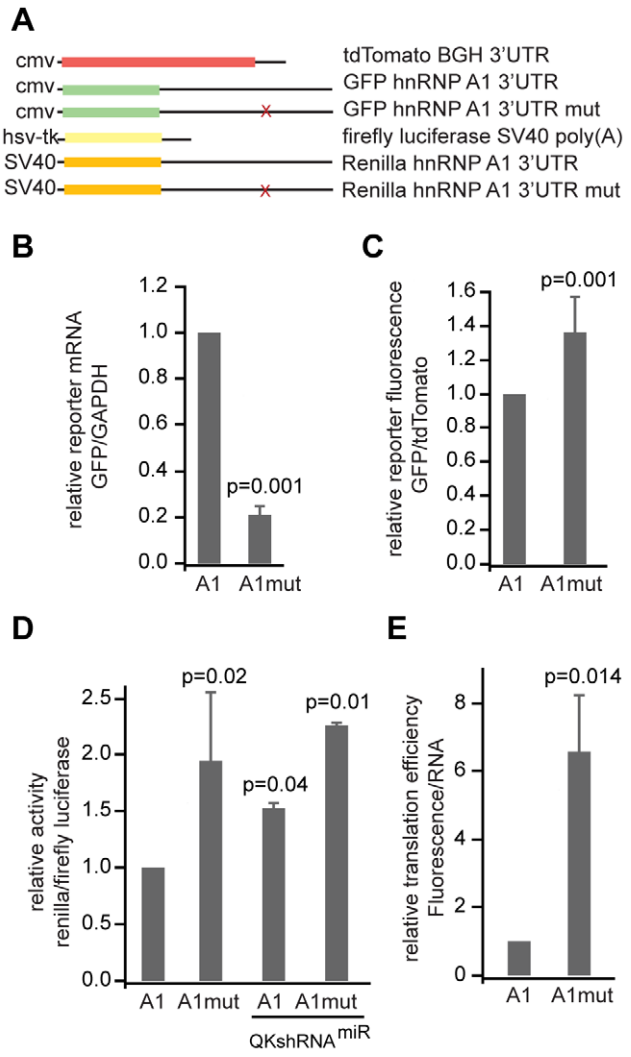

Figure 3. QK controls reporter expression through the QSBE in the *Hnrnpa1* 3′ UTR. (A) Constructs used in reporter assays. The *Hnrnpa1* 3′ UTR or the *Hnrnpa1* 3′ UTR with the U to G point mutation was inserted into the 3′ UTR of phrGFPII-1. tdTomato was unmodified and served as a transfection control. For the luciferase assays, the firefly luciferase transfection control was encoded on the same plasmid as the experimental *Renilla* luciferase. The wild type or mutant *Hnrnpa1* 3′ UTR was cloned behind *Renilla*. (B) Two color fluorescence reporter assays conducted with the *Hnrnpa1* 3′ UTR and the U-to-G QSBE point mutation. (B) RNA level and (C) reporter fluorescence were assayed as in Figure 1. The RNA data represent the average and standard deviation of nine replicates from three independent experiments. The fluorescence data represent the average and standard deviation of 27 replicates from 9 independent experiments. (D) Dual luciferase reporter experiments, where the wild type or U-to-G point mutant *Hnrnpa1* 3′ UTR was inserted into the 3′ UTR of *Renilla reniformis* luciferase, and Firefly luciferase expressed from the same vector served as a transfection efficiency control. The dual reporter was transfected into CG-4 cells or a CG-4 cell line that stably expresses a *Qk* shRNA^{miR}. The relative activities of firefly and *Renilla* luciferase were determined using a plate reader. Error bars indicate the standard deviation of five independent replicates for the CG-4 cells or variance of two replicates for the shRNA^{miR} cell line. (E) GFP reporter translational efficiency was determined by dividing the relative amount of reporter protein by the relative amount of reporter mRNA. The error was propagated from the standard deviations in (B) and (C) as in Figure 1 and as described in methods.
doi:10.1371/journal.pgen.1001269.g003

brains of Qk^{qk} mice for three myelin-related transcripts: *Mbp*, *Plp1*, and *Mag*. We therefore selected these mRNAs for further analysis.

For *Mag*, we analyzed the ratio of *S-Mag*, which includes the alternatively spliced exon 12, to *L-Mag*, in which the exon is skipped. Inclusion of this exon is increased in Qk^{qk} mice despite the overall reduction of QK in each [14,16]. Control CG-4 cells transfected with the GFP plasmid and selected in G418 contained an *S-Mag* to *L-Mag* isoform ratio of 2.4±0.2 (Figure 5A). Reduction of QK with *Qk* siRNA caused an increase in the amount of *S-Mag* compared to *L-Mag*, resulting in an isoform ratio of 4.7±1.2 ($p = 0.04$, Figure 5A, 5C). The increase is similar to that previously observed by others in the Qk^{qk} mouse brain, confirming that QK controls *Mag* splicing in CG-4 cells as it does in brains. CG-4 cells transfected with *Hnrnpa1* siRNA displayed an increased isoform ratio of 5.0±1.7 ($p = 0.01$) (Figure 5A, 5C). The direction of the change is consistent with a role for hnRNP A1 in splicing repression and with our observation that QK has a net positive effect on hnRNP A1 expression in CG-4 cells. Transfection with control, *Hnrnpc*, or *Sfrs5* siRNAs did not significantly alter the isoform ratio (Figure 5A, Figure S4). The data indicate that hnRNP A1 regulates *Mag* exon 12 splicing and suggest that QK control of *Mag* splicing may be indirect.

We also examined alternative splicing of *Plp1* and *Mbp*. RT-PCR analysis of *Mbp* alternative splicing did not reliably confirm the QK-dependence in CG-4 cells (data not shown). To further examine *Plp1* splicing in QK knockdown and in hnRNP A1 knockdown CG-4 cells, RT-PCR primers were designed to determine the relative ratio of *Plp1*, which contains a longer exon 3 variant due to alternative 5′ splice site selection, to *Dm20*, a transcript containing the shorter exon 3 variant. While QK siRNA reduced the amount of *Plp1* compared to *Dm20*, mirroring the change observed in Qk^{qk} mouse brains, there was no detectable change upon transfection with *Hnrnpa1* siRNA (Figure 5B, 5C). The data suggest that for *Plp1*, QK controls alternative splicing not through hnRNP A1 but, instead, through some other mechanism.

Microarray assay design

Because QK positively regulates hnRNP A1 in CG-4 cells, we anticipated that the isoform ratio of many transcripts in addition to *Mag* and *Plp1* would be altered upon QK knockdown. To test this hypothesis, we used Affymetrix 1.0 ST exon microarrays to assess global changes in gene expression in response to QK depletion (Figure 6A). To reduce the likelihood of detecting off-target effects or changes in gene expression brought about by the clonal selection procedure, we also analyzed cells that were prepared by transient transfection with *Qk* siRNA (Ambion) along with a GFP-expressing plasmid that allows selection with a different drug than that used for stable cell line production. After two days of selection, the *Qk* siRNA reduces *Qk* expression by approximately 80%, while the control siRNA does not (Figure 6B). In parallel, we also analyzed changes caused by depleting hnRNP A1 by transient transfection of a corresponding siRNA. Depletion of hnRNP A1 was confirmed by Western blotting (Figure 6C). Three independent biological replicates were analyzed for each group. In addition to the *Qk* shRNA, *Qk* siRNA, and *Hnrnpa1* siRNA groups, we also assayed gene expression in control cells treated with non-silencing shRNA, non-silencing siRNA, and untreated CG-4 cells.

Identification of transcripts controlled by QK in oligodendrocyte precursors

We first wished to identify the set of transcripts regulated by QK at the level of transcript abundance. At a False Discovery Rate (FDR) of 0.1 (step-up, p-value 0.0012), 224 transcripts were identified with a p-value at or below the cut-off (Figure 7A, Table

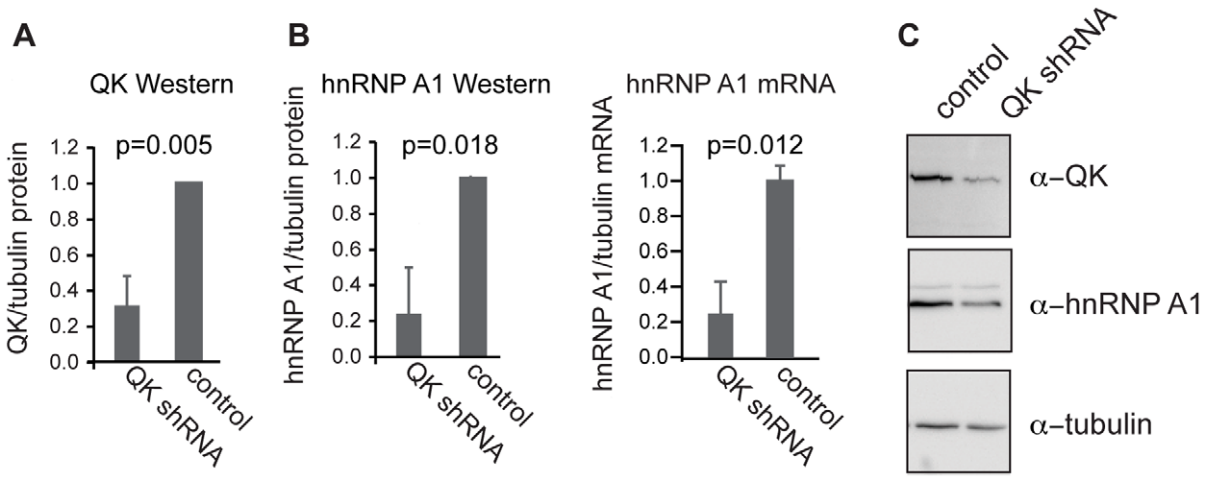

Figure 4. QK regulates expression of endogenous *Hnrnpa1*. (A) QK protein was reduced in a CG-4 cell line stably transfected with a construct expressing a *Qk* shRNA^{miR} compared to a control line expressing a nonsilencing shRNA^{miR}. (B) hnRNP A1 protein was detected by Western blotting and *Hnrnpa1* mRNA was detected by real time RT-PCR. Both protein and mRNA were reduced in the QK knockdown line compared to the control line. Tubulin served as a loading control for both assays. (C) Representative Western blot images for the data presented in (A) and (B). Error bars indicate the standard deviation of at least three replicates.
doi:10.1371/journal.pgen.1001269.g004

S1). These transcripts are predicted to include 22 false positives and 202 true positives. For this set of transcripts, the mean expression of the three replicates was calculated and the $\log_2$ fold change compared to untreated CG-4 cells was determined.

Hierarchical clustering (Pearson's dissimilarity, centroid method) revealed that gene expression in the *Qk* siRNA and *Qk* shRNA samples was highly correlated (Pearson's correlation coefficient 0.88; Figure 7A), confirming our statistical selection of transcripts. Gene expression changes in the control samples were less correlated, indicating that we have identified changes in gene expression due to the reduction of QK and not to other elements of the experimental protocol. To confirm the array results, we used quantitative RT-PCR to assess gene expression changes in the *Qk* shRNA^{miR} stable cell line. Of fourteen transcripts tested, thirteen had a difference in expression by quantitative RT-PCR (Figure 7B). The transcript that had the greatest change in QK knockdown cells was the previously identified QK target *Mbp* (Figure 7B).

Gene ontology analysis revealed that myelin components were significantly enriched, as predicted from the role of QK in myelination (Table 1). Furthermore, the top ten decreasing transcripts include two myelin components, *Mbp* and *Plp1* (Figure 7B). Other enriched categories include epidermal growth factor and acetylcholine receptor activities and tau protein function, suggesting a widespread disruption of processes that promote myelination. Epidermal growth factor receptor activity has been shown to promote myelination in the mouse, while acetylcholine receptor activity promotes oligodendrocyte survival [37,38]. The tau pathway has been linked to oligodendrocyte process formation [39].

A subset of QK targets are co-regulated by hnRNP A1

We next wished to compare the effects of reducing hnRNP A1 with the effects of reducing QK genome-wide. We identified probesets with a significant change in expression upon QK knockdown using an FDR set at 0.1 (step up, p-value 0.00012). Hierarchical clustering (Pearson's dissimilarity, centroid method) demonstrated that the probeset expression changes in *Hnrnpa1* siRNA treated cells clustered closely to those in *Qk* siRNA treated cells (correlation coefficient 0.81) (Figure 7C). *Qk* shRNA and *Qk* siRNA also clustered closely, as one would predict (correlation coefficient 0.91) (Figure 7C). The correlation between expression changes in the *Hnrnpa1* siRNA and *Qk* knockdown groups was independent of the False Discovery Rate (Figure S5). The data indicate that there is similarity in the probeset level changes in gene expression between the *Qk* knockdown and *Hnrnpa1* knockdown samples genome-wide.

We repeated our analysis at the whole transcript level, selecting transcripts regulated by QK (FDR 0.1) and performing the same analysis as for probesets. Again, there is a strong correlation at the whole transcript level between expression changes in the *Hnrnpa1* siRNA and the *Qk* siRNA samples (Pearson's correlation coefficient 0.83) (Figure S6). This correlation is of a similar magnitude to the correlation we observe between *Qk* shRNA and *Qk* siRNA (Pearson's correlation coefficient 0.88). These data suggest that QK and hnRNP A1 exert similar pressures on gene expression and alternative splicing on a genome-wide scale in oligodendrocyte precursors.

hnRNP A1 motifs are enriched in QK-responsive exons

hnRNP A1 is a sequence-specific RNA binding protein that regulates the isoform ratio of transcripts that contain a binding site in or near exons that are alternatively spliced [40–42]. It binds to several sequence variants, including the SELEX-derived UAGGG(A/U) as well as UAGGU and related sequences [43,44]. Our observation that QK regulates *Hnrnpa1* expression predicts that hnRNP A1 binding sites will be present in the vicinity of QK-responsive exons.

In order to obtain a set of exons predicted to be alternatively spliced upon *Hnrnpa1* or *Qk* knockdown, we re-analyzed our microarray data using AltAnalyzer [45] and the full Affymetrix probeset annotation. The analysis identified both upregulated and downregulated exons in both data sets. For *Qk* knockdown CG-4 cells, 78 exons were downregulated and 219 were upregulated, and for *Hnrnpa1* knockdown cells, 93 exons were downregulated 70 were upregulated.

To identify enriched motifs, we determined the frequency of all 5mers contained in the sequences of regulated exons relative to

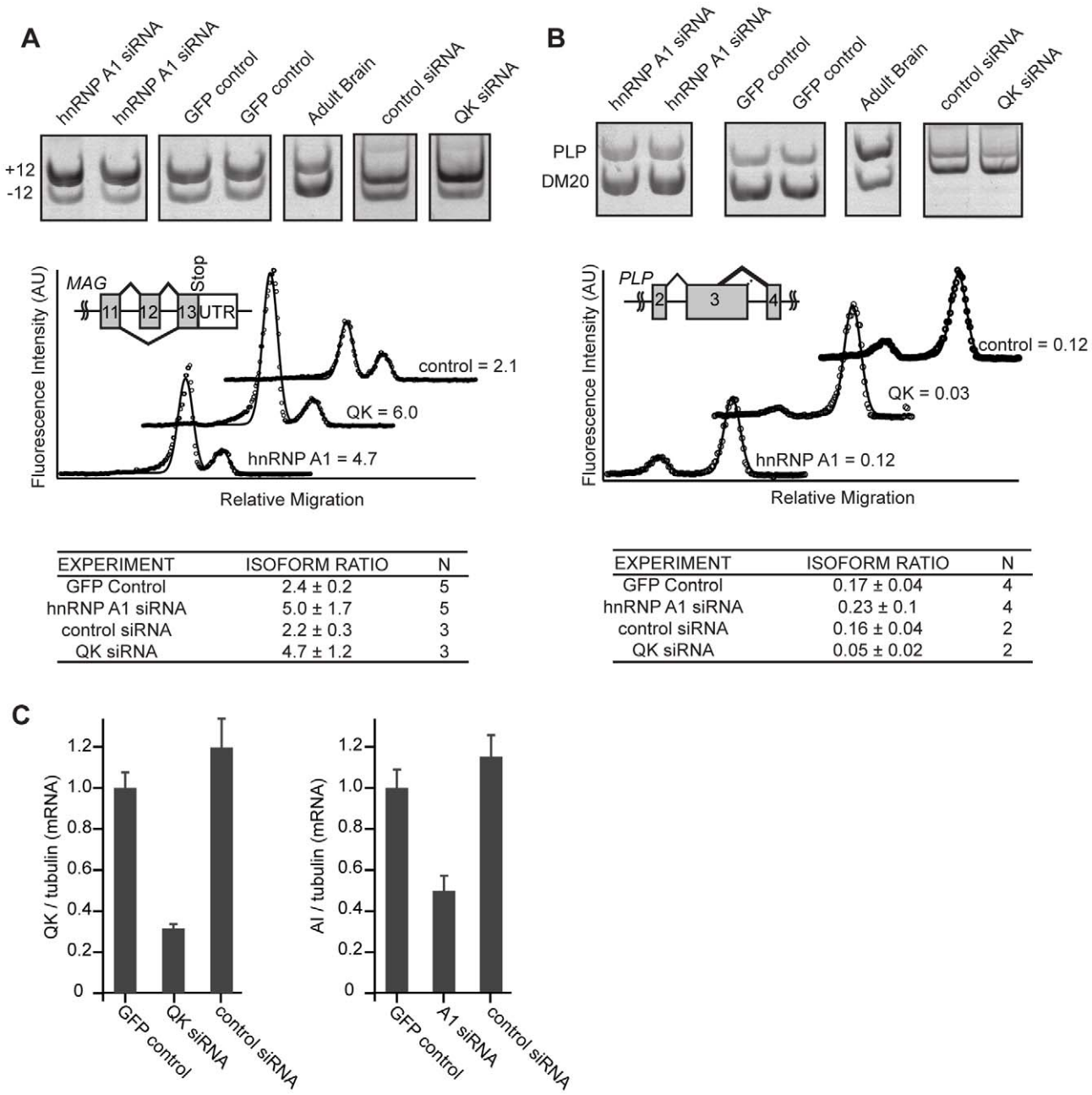

EXPERIMENT	ISOFORM RATIO	N
GFP Control	2.4 ± 0.2	5
hnRNP A1 siRNA	5.0 ± 1.7	5
control siRNA	2.2 ± 0.3	3
QK siRNA	4.7 ± 1.2	3

EXPERIMENT	ISOFORM RATIO	N
GFP Control	0.17 ± 0.04	4
hnRNP A1 siRNA	0.23 ± 0.1	4
control siRNA	0.16 ± 0.04	2
QK siRNA	0.05 ± 0.02	2

Figure 5. hnRNP A1 co-regulates *Mag* alternative splicing. (A) RNA was prepared from cells that had been transiently transfected with *Hnrnpa1* or *QK* siRNA and selected with G418. RNA produced from CG-4 cells transfected with a control selection plasmid was analyzed alongside as a control. Isoforms of *Mag* containing or lacking exon 12 were amplified by RT-PCR using fluorescent primers. Products were separated in 5% acrylamide gels. Gels were scanned and the relative isoform ratio was calculated from the intensity profile of the lane using ImageGauge. Representative intensity profiles are presented below representative gel images. Data and standard deviations were calculated from 3 (control siRNA and *Qk* siRNA) or 5 (GFP control and *Hnrnpa1* siRNA) independent transfections. An increase in expression of the longer isoform was detected upon transfection of both *Hnrnpa1* and *Qk* siRNA. (B) *Plp1* and *Dm20* isoform ratios were analyzed as described above for *Mag*. A decease in expression of the upper isoform was detected when *Qk* siRNA was transfected but not when *Hnrnpa1* siRNA was transfected. (C) *Qk* and *Hnrnpa1* knockdown were confirmed by qRT-PCR.
doi:10.1371/journal.pgen.1001269.g005

their frequency in all annotated rat exons (Table S2). To assess statistical significance, we also determined the 5mer frequency from ten sets of an equivalent number of randomly selected exons. Significantly changed 5mers were identified based upon criteria of a greater than 1.5 fold enrichment and a p-value of less than 0.05 when compared to the randomly selected exon set (Table S2). We found a significant enrichment over random of 42 5mers in QK upregulated exons, including the hnRNP A1 motif TAGGT (fold enrichment FE = 1.54, $p = 5 \times 10^{-3}$) and the QSBE motif ACUAA (FE = 1.54, $p = 8 \times 10^{-7}$, Figure 8A). The A1 motif is similar to an exonic splicing silencer motif identified by Burge and co-workers [46]. There are 149 significant enriched 5mers in QK downregulated exons. These include the hnRNP A1 motif TAGGT (FE = 1.94, $p = 3 \times 10^{-3}$), but not the QSBE ACUAA motif. While

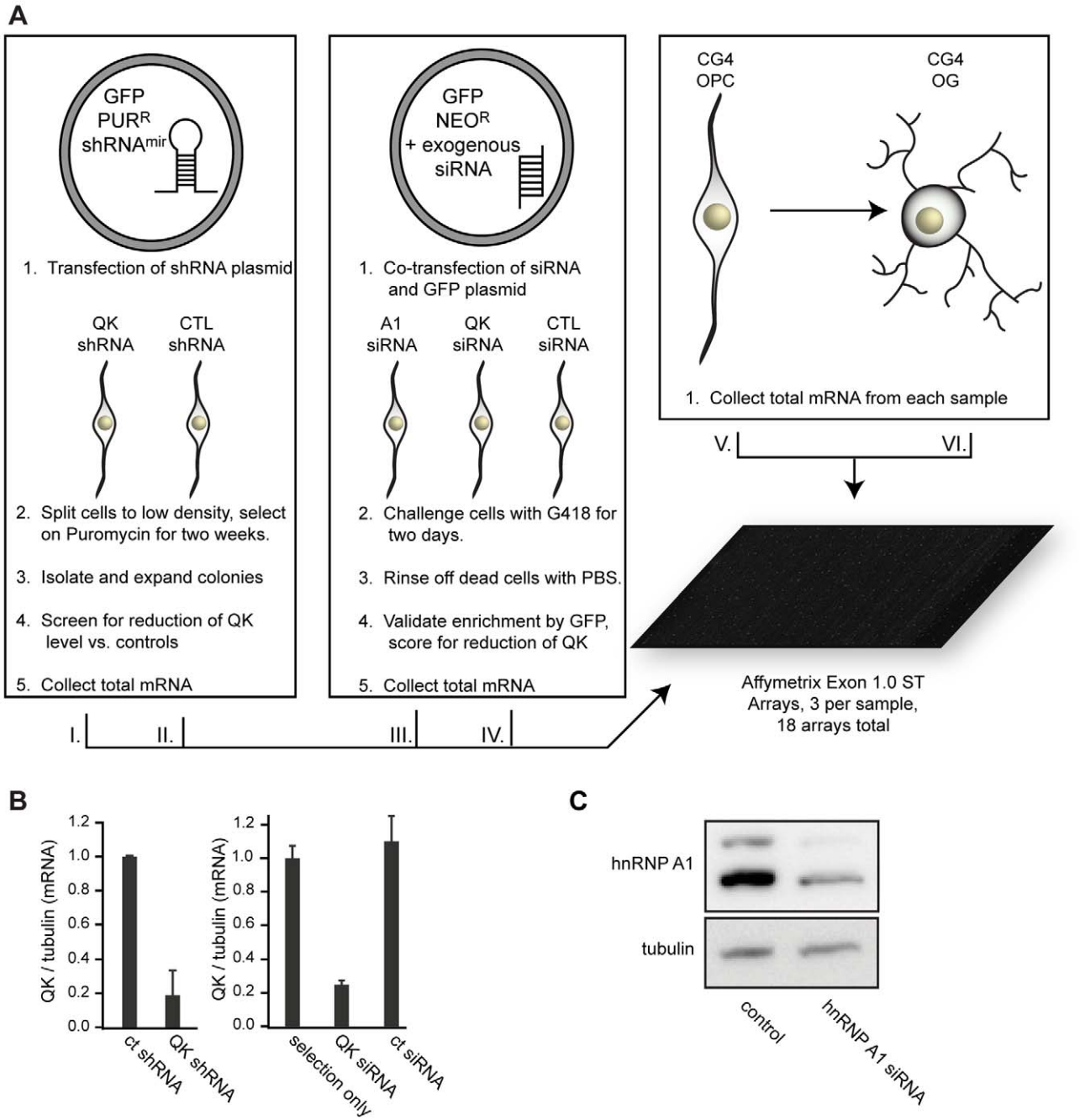

Figure 6. Microarray assay design. (A) Diagram of knockdown cell populations and controls. QK was reduced with *Qk* shRNA^{miR} and *Qk* siRNA. hnRNP A1 was knocked down with siRNA. Control samples consisted of untransfected CG-4 cells, CG-4 cells transfected with nonsilencing siRNA, stably transfected CG-4 cells expressing a nonsilencing shRNA^{miR}, and differentiated CG-4 cells. Each group was assayed in triplicate using three biological replicates. (B) Real time RT-PCR demonstrating QK reduction in the *Qk* shRNA^{miR} stable cell line and in CG-4 cells transiently transfected with *Qk* siRNA. Data are the mean of three replicates +/− standard deviation. Error was propagated from the *Qk* and *Tubulin* standard deviations. (C) Western blot demonstrating hnRNP A1 knockdown in CG-4 cells.
doi:10.1371/journal.pgen.1001269.g006

this motif is enriched relative to all exons, the average of the randomly selected exons also yields a significantly changed p-value. As expected, hnRNP A1 motifs were also enriched in the hnRNP A1 knockdown cells (Figure 8A: upregulated exons; TAGGT, FE = 2.32, $p = 4\times10^{-6}$; downregulated exons: TAGGT, FE = 2.2, $p = 4\times10^{-4}$; TAGGG, FE = 2.5, $p = 1.7\times10^{-5}$). The enrichment of the hnRNP A1 motif in QK-responsive exons suggests that many but not all QK-dependent alternative splicing events are mediated indirectly by hnRNP A1. The enrichment of the QK motif is consistent with a direct role for QK in the regulation of some alternative splicing events.

Discussion

The RNA binding protein QK controls myelination by governing the stability, subcellular localization, and alternative

A

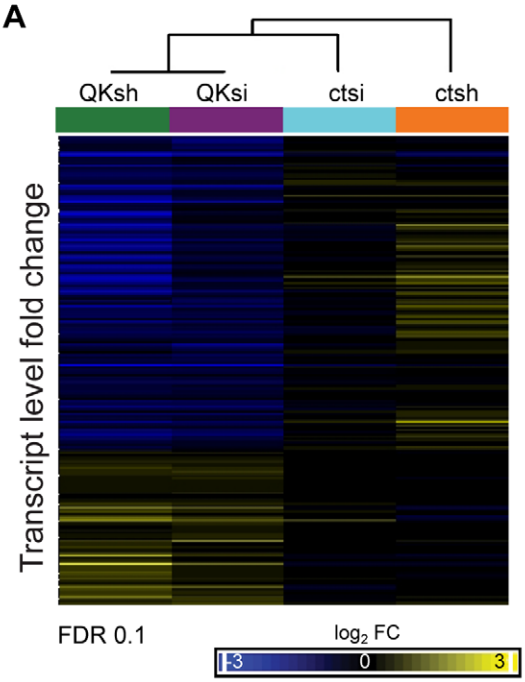

Correlation Coefficients

QK siRNA vs. QK shRNA 0.88	
ct siRNA vs. ct siRNA	0.27
ct shRNA vs. QK shRNA	-0.41
ct siRNA vs. QK siRNA	0.34

B

Gene Symbol	log2 fold change microarray	pcr
abat	-2.0	-2.0
cnp	-1.7	-1.3
dlgh3	-0.8	-1.4
egr1*	4.9	5.6
egr3	2.4	2.5
erbb4	-1.1	-0.5
gas7	-1.8	-2.7
itm2b*	-1.8	-0.3
mbp	-3.4	-4.6
ncam2	-1.5	-1.3
ndrg2	-2.0	-0.8
plp1	-2.6	-4.2
pnlip	-2.8	-3.2
sirt2	-1.0	-1.1

*p values for these transcripts were between the cutoff and 0.05

C

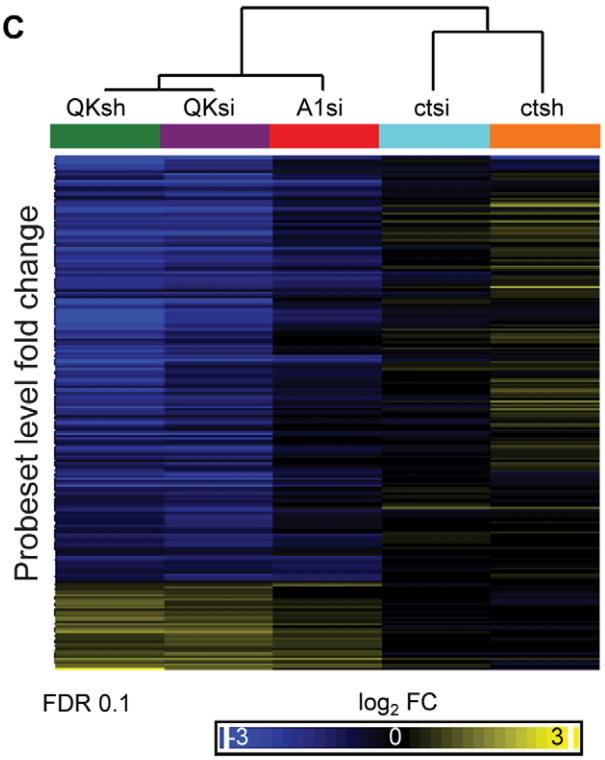

Correlation Coefficients

QK siRNA vs. QK shRNA	**0.91**
A1 siRNA vs. QK siRNA	**0.81**
A1siRNA vs. QK shRNA	**0.74**
QK siRNA vs. control siRNA	0.17
A1 siRNA vs. control siRNA	0.36
control shRNA vs control siRNA	-0.12

Figure 7. Identification of the QK and hnRNP A1 regulatory networks in CG-4 cells. (A) Hierarchical clustering demonstrated high correlation in the gene expression changes between the two knockdown populations. Transcripts altered by QK depletion were identified using a two sample t-test and an FDR of 0.1 (p-value cutoff 0.0012). For the selected transcripts, the expression values of the three biological replicates were averaged and the fold change compared to untransfected CG-4 cells was calculated. The resulting values were clustered (Pearson's dissimilarity, centroid method), and correlation coefficients were calculated. (B) Real time PCR confirmation of microarray results. RNA was extracted from the *Qk* shRNA^{miR} knockdown cell line and from the nonsilencing shRNA^{miR} control cell line. Real time PCR was performed in triplicate. Expression values were normalized to tubulin as a loading control. Data are the mean of three replicates, expressed at log2 for comparison to the microarray results. (C) QK-dependent probeset expression changes are highly correlated with probeset expression changes caused by hnRNP A1 depletion. Individual probesets with expression changes in response to QK knockdown were identified using a two-sample t-test, comparing the knockdown groups to the control groups. The mean of each group was determined and the difference from the CG-4 cell line was calculated. Values were clustered as in (A). Correlation coefficients were calculated using Partek GS software. Probesets were selected for clustering based solely on their change in the QK knockdown samples.

doi:10.1371/journal.pgen.1001269.g007

Table 1. Top 10 enriched gene ontology terms in QK knockdown samples.

Function	Enrichment Score	% genes in pathway that are present	GO ID
acetylcholine receptor regulator activity	21.9556	100	30548
response to organic nitrogen	19.1296	33.3333	10243
positive regulation of synaptic transmission	13.2249	33.3333	50806
regulation of transmission of nerve impulse	12.7344	12.6214	51969
myelin sheath	12.5974	42.8571	43209
epidermal growth factor receptor binding	12.5974	42.8571	5154
receptor regulator activity	12.5974	42.8571	30545
positive regulation of transmission of nerve impulse	12.3089	30.7692	51971
tau protein binding	11.989	66.6667	48156
tau-protein kinase activity	11.989	66.6667	50321

*Transcripts selected at FDR 0.2.
doi:10.1371/journal.pgen.1001269.t001

splicing of a specific set of myelin-related mRNAs. Relatively few direct QK targets have been characterized, and the mechanism by which QK regulates such diverse processes is unclear. Here, we show that the QSBE sequence—the primary determinant for high affinity QK binding—is required for regulation of *Mbp* mRNA. Moreover, we show that QK directly regulates the transcript encoding the splicing factor *Hnrnpa1* through a conserved QSBE in its 3′ UTR. The strong correlation between the changes in transcript and probeset abundance upon *Qk* or *Hnrnpa1* knockdown is consistent with a vertical regulatory relationship and suggests that hnRNP A1 is a primary effector of QK function.

The reporter data reveal that QK has two opposing effects on *Mbp* and *Hnrnpa1* expression, positively regulating mRNA abundance while negatively regulating translational efficiency. The mode of regulation is consistent with a model where QK stores its targets in a translationally quiescent but stable complex. Such a regulatory scheme would enable a transient burst of translation in response to a signal that releases QK from its targets, such as phosphorylation. Consistent with this hypothesis, Feng and co-workers have shown that QK activity is regulated by tyrosine phosphorylation and that the level of phosphorylation is modulated during myelination [47].

The microarray analysis described herein delineates the set of transcripts controlled by QK in the CG-4 oligodendrocyte precursor cell line. The most dramatically changed transcript is the previously characterized QK target *Mbp* [10,13]. We have also observed striking changes in the expression of several other important myelin genes, suggesting that QK has broad control of transcripts important for myelination. For example, *Cnp1* has been implicated in maintaining the integrity of myelinated axons [1]. *Fyn* stimulates *Mbp* transcription, suggesting control of *Mbp* expression by QK is both direct and indirect [48]. Finally, UDP glycosyltransferase 8 (Ugt8) produces myelin sphingolipids, suggesting that QK controls synthesis of the lipid components of myelin as well.

Several labs have demonstrated that hnRNP A1 is a post-transcriptional regulator of gene expression. hnRNP A1 represses alternative splicing when associated with silencing elements near spice sites [40–42]. Additional functions have also been proposed. hnRNP A1 also binds to telomeric DNA, where it is thought to promote telomere elongation [49]. Furthermore, hnRNP A1 is implicated in the Drosha-mediated processing of a primary microRNA [50,51]. It will be interesting to determine whether the effects of QK on gene expression in oligodendrocyte precursors are mediated by hnRNP A1 through any of these mechanisms.

The data also have implications for the mechanism by which hnRNP A1 regulates *Mag* alternative splicing. An hnRNP A1 motif is present in *Mag* intron 12 immediately downstream of the 5′-splice site (Figure 8B), suggesting a model in which binding of hnRNP A1 to this motif blocks 5′-splice site recognition, promoting skipping of exon 12. Consistent with this model, our data and the work of others show that reduction of QK or hnRNP A1 increases MAG exon 12 inclusion [14]. Moreover, a point mutation in this hnRNP A1 binding motif has been shown to cause constitutive exon 12 inclusion [14], although we note that this mutation also strengthens the 5′-splice site consensus, which confounds a simple interpretation of this result.

The microarray analysis suggests that some of the effects of QK on splicing may be indirect. In line with these observations, screening the 3′ UTRs of the QK responsive transcripts using the sequence analysis tool Patscan [52] reveals that under a third contain the sequence element required for QK binding (Table S3). Together, these observations suggest numerous indirect changes in gene expression caused by QK depletion. Consistent with this hypothesis, we observe enrichment of 5mer motifs that do not correspond to QK or hnRNP A1 binding motifs in QK-responsive exons (Table S2). These may represent binding sites for other RNA regulators.

Understanding how QK controls its network of transcripts will require a detailed analysis of directly bound QK targets in oligodendrocyte lineage cells. Use of the cross-linked immunoprecipitation technique [53–56] should greatly facilitate such an analysis. A recent study used a variant of the technique, in which chemically modified nucleotides were incorporated into mRNAs in HEK293 cells overexpressing QK to enhance crosslinking [27]. Despite the fact that the mRNAs expressed in HEK293 are likely to be substantially different from those expressed in oligodendrocyte lineage cells, 20% of the transcripts identified in our microarray analysis are present the list of crosslinked transcripts, more than the 11–13% overlap when the list of transcripts crosslinked to Pumilio 2 or TNRC6 are analyzed as controls.

Numerous studies have implicated *QKI* and other myelin genes in SCZ. Thirty-eight genes that have been implicated in SCZ [57] are affected by *Qk* knockdown, including *CNP*, *MBP*, *PLP1*, and *OMG* (Table S4). Additionally, SCZ brains have similar splicing defects to those observed in association with *Qk* knockdown, including changes in *MAG*, *NCAM*, and *ERBB4* [16,21,58]. Thus,

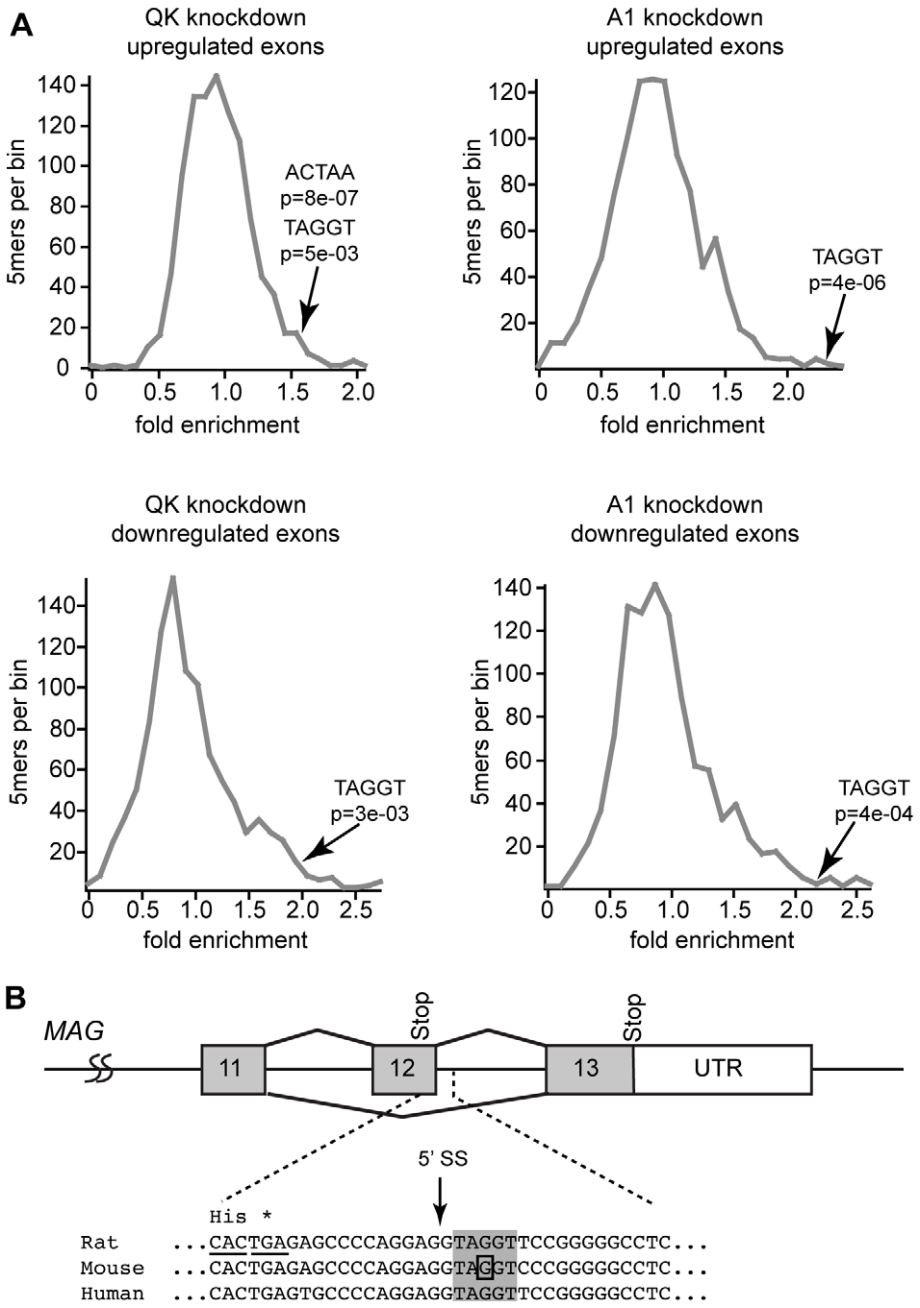

Figure 8. hnRNP A1 motifs are enriched in QK-responsive exons. (A) Relative 5mer frequencies in exons that change in response to QK or hnRNP A1 knockdown were binned according to fold enrichment compared to frequency in all exons. The position of hnRNP A1 and QK motifs is annotated by an arrow. The significance of the enrichment was determined by comparison to 5mer fold enrichment in ten groups of an equivalent number of exons selected at random. (B) An hnRNP A1 motif (gray box) is present in *Mag* intron 12 immediately downstream of the 5′-splice site (arrow). The position of the mutation that causes constitutive *Mag* exon 12 inclusion is boxed [14].
doi:10.1371/journal.pgen.1001269.g008

the changes in gene expression observed by microarray analysis may provide a link between QKI function and disease.

Gene dosage effects have been implicated in many other human diseases. For example, Pelizaeus-Merzbacher disease is associated with *PLP1* duplication [59]. Intriguingly, copy number variation has been linked to schizophrenia, Charcot-Marie-Tooth disease, and autism, suggesting that small variations in the dosage of important myelin related genes can have significant clinical outcome [60–62].

In summary, we have identified a new direct QK target, the *Hnrnpa1* transcript, in oligodendrocyte lineage cells. Additionally, we have identified the set of transcripts directly or indirectly controlled by QK and have shown that hnRNP A1 co-regulates part of this set. The results suggest that the importance of QK for myelin formation lies not only in the identity of major direct targets, but also in the network of secondary targets under QK control. They also demonstrate that QK is a prime regulatory factor controlling gene expression in oligodendrocyte precursors

and that hnRNP A1 is a large contributor to its effects on alternative splicing.

Materials and Methods

Ethics statement

Brain tissue was harvested from mice in accordance with protocols approved by the University of Massachusetts Medical School Institutional Animal Care and Use Committee. The animal care program complies with Federal and State laws and the PHS policy on Humane Care and Use of Laboratory Animals. The experiments were designed in order to minimize the number of animals used.

Cell culture and transfections

The CG-4 rat oligodendrocyte precursor and B104 cell lines were a gift from Lynne Hudson and were cultured according to Louis et al. [29]. CG-4 cells were maintained as undifferentiated progenitors in the presence of 30% B104 conditioned medium for the duration of the assays except as noted otherwise. Cells were transfected with Lipofectamine 2000 (Invitrogen) according to instructions from the manufacturer. Where indicated, 24 hours after transfection, transfected CG-4 cells were selected by incubation with 1500 ng/µl G418 (Geneticin, Invitrogen) for 48 to 72 hours.

To generate stable cell lines, cells were transfected as above with the indicated shRNA^{miR} constructs (Open Biosystems). After 24 hours, cells were trypsinized and plated sparsely on 150 mm plates in the presence of 2 ng/µl puromycin. Cells were allowed to proliferate for approximately two weeks, until colonies had formed. Colonies were picked and transferred into 24 well plates to proliferate.

Plasmids and siRNAs

The *Hnrnpa1* 3′ UTR (RefSeq NM_0104447) was cloned into the phrGFPII-I plasmid (Strategene) after PCR amplification from an *Hnrnpa1* full length I.M.A.G.E. clone (Invitrogen). The T to G mutation in the QSBE was introduced by QuikChange site directed mutagenesis (Stratagene). Sequences of all constructs were confirmed by sequencing. tdTomato was provided by Roger Tsien and colleagues [63]. To generate a construct for expressing tdTomato in mammalian cells, the tdTomato coding sequence was excised from the original plasmid and cloned into the pcDNA 3.1+ expression vector (Invitrogen). The vector psiCheck 2 was a gift from Phil Zamore. The *Hnrnpa1* wild type and mutant UTRs were cloned from the GFP expression vectors into psiCheck2.

Qk siRNA1, *Hnrnpa1* siRNA, and the non-targeting control siRNA were commercially designed (Ambion). The *Qk* pGIPZ shRNA^{miR} (Open Biosystems) was obtained from the University of Massachusetts RNAi core facility.

Reporter assays

For the fluorescent reporters, CG-4 cells were seeded onto the surface of a 24 well plate and, after 24 hours, transfected with 0.6 µg of the plasmid encoding GFP with or without a UTR of interest and 0.1 µg of the tdTomato control plasmid using Lipofectamine 2000 (Invitrogen). Complexes were formed in medium without antibiotic or other supplements. Transfections were done in DMEM containing N1 supplements, biotin, insulin, L-glutamine, but without antibiotic or B104 conditioned medium. After 24–48 hours of incubation at 37°C, the plate was read using a Victor3 plate reader (Perkin Elmer). GFP was excited using a 485 nm filter and detected through a 519/20 filter. tdTomato was excited using a 531/25 nm filter and detected through a 580/10 filter. All filters were purchased from Chroma. Each well was read 25 times, in a 5 by 5 grid with 0.1 mm spacing between the spots. The well average was computed from these 25 spots. GFP fluorescence was divided by tdTomato fluorescence to control for transfection efficiency and cell density. Three or four independently transfected wells were averaged for each experiment and the standard deviation was calculated.

For the luciferase reporters, cells were transfected as above with the plasmid psiCheck2 (Promega) or a cloned psiCheck2 variant with the hnRNP A1 wild type or T to G mutant 3′ UTR cloned behind Renilla. 24–48 hours after transfection, cells were lysed in 150 µl of lysis buffer per well and dual luciferase assays were conducted using the Dual Luciferase Assay System (Promega) according to the manufacturer's instructions.

RNA binding assays

For the gel shift assays, recombinant QK was purified as previously described [25]. RNA gel shifts and fluorescence polarization assays were performed according to [64], with the exception that electrophoresis was carried out in a non-denaturing 5% polyacrylamide slab gel in 1xTBE buffer. RNA co-IPs from uncrosslinked lysates were conducted according to Tenenbaum et al. [65], using brains from C57BL/6 mice. Formaldehyde crosslinking of mouse brain tissue and immunoprecipitation from crosslinked lysate was conducted as described in [66]. After crosslink reversal, RNA was extracted with Trizol reagent according to the manufacturer's instructions, the purified RNA was treated with DNase (Ambion Turbo DNAfree), and co-precipitated RNA was amplified by one step RT-PCR (Invitrogen) with transcript specific primers. Antibodies to QK (Bethyl labs) and 6xHisG (Invitrogen) were commercially obtained. PCR primers were fluorescently labeled at the 5′ end unless otherwise noted. After separating the PCR product from free primers by agarose gel electrophoresis, gels were imaged on a Fuji FLA-5000 using a blue laser.

Quantitative PCR

RNA was extracted from cultured cells with Trizol Reagent (Invitrogen) and treated with Turbo DNAfree (Ambion) or RQ1 DNase (Promega) according to the provided instructions. The yield was determined by spectrophotometry. Real time RT-PCR was performed using a one-step RT-PCR kit (Qiagen or Bio-Rad) according to the manufacturer's instructions and cycled on an Opticon thermal cycler (Bio-Rad). All assays were performed in triplicate. For each target the presence of a single product after cycling was confirmed by agarose gel electrophoresis. Data were analyzed by comparison to a 5-point standard curve constructed at the time of cycling or according to the method of Rutledge [67]. GAPDH or tubulin and tdTomato were used for normalization as indicated in the figure legends.

Splicing assays

CG-4 cells were transfected as for the dual color fluorescence reporter assay, using 20 nM siRNA and 0.3 µg GFP-selection plasmid per well. After 24 hours, the medium was replaced with 30% B104 conditioned medium containing 1500 ng/µl Geneticin (Invitrogen). Cells were incubated in the selection medium for 48 hours, then washed two times with PBS. RNA was isolated with Trizol (Invitrogen). PCR was conducted with 5′ fluorescein labeled primers and the products were isolated on a non-denaturing 5% polyacrylamide gel. Gels were imaged on a Fuji FLA-5000 imager using a blue laser. Band intensity in each lane was quantified using ImageGauge profile analysis.

Microarrays

CG-4 cells were grown and transfected as described above. RNA was extracted in Trizol (Invitrogen). RNA was further purified and genomic DNA was eliminated using the RNEasy Plus mini kit (Qiagen). Knockdown of *Qk* or *Hnrnpa1* was verified by quantitative RT-PCR. Rat Exon 1.0 ST microarrays were obtained from Affymetrix. Three independent biological replicates were assayed per group. Sample labeling and array hybridization were conducted by the University of Massachusetts Genomics Core Facility according to Affymetrix procedures. Data were analyzed with Partek GS, using the Affymetrix extended probeset annotation with a GC background correction RMA algorithm. Differentially expressed mRNAs and probesets were identified using a two-sample t-test, with an FDR of 0.1 unless otherwise noted. For analysis of the *Hnrnpa1* knockdown groups, probesets and transcripts that significantly changed in response to QK depletion were selected, then the changes in expression in response to hnRNP A1 depletion were clustered alongside the other control and experimental groups.

Statistical analyses

All assays were performed in triplicate unless otherwise indicated. Error bars represent the standard deviation of the experimental replicates. P-values were calculated from a two-sample t-test assuming unequal variance. Errors were propagated from the individual standard deviations according to the formula $\Delta Z = Z(SQRT(((\Delta A/A)\hat{}2)+((\Delta B/B)\hat{}2)))$ where $Z = A/B$.

5mer enrichment analysis

The sequences of regulated exons were obtained from Affymetrix. Exons from all rat genes were obtained from the UCSC genome browser. The frequency of 5mers in each exon was determined using Perl scripts. Random sets of exons were selected using Perl scripts. The average and standard deviation of 5mer frequency were calculated for the random sets of exons to obtain a p-value for fold enrichment significance.

Supporting Information

Figure S1 Two color fluorescence reporter assay. (A) CG-4 cells transfected with GFP, tdTomato, or co-transfected with both could be distinguished based upon red and green fluorescence. (B) CG-4 cells co-transfected with GFP and tdTomato plasmids exhibited both red and green fluorescence. (C) Red and green fluorescence could be distinguished with virtually no bleed through between the fluorescence channels.
Found at: doi:10.1371/journal.pgen.1001269.s001 (0.80 MB TIF)

Figure S2 QK does not interact with the *Mag* QASE or the *Plp1* ESE. (A) The *Mag* intron 12 QASE and the *Plp1* exon 3 ESE do not contain the high affinity QK binding element ACUAA or the related sequence AUUAA. (B) The *Mag* QASE and the *Plp1* ESE do not bind QK with high affinity in vitro. Three overlapping fragments of the QASE or the ESE sequence, diagramed in (A), were equilibrated with recombinant QK in vitro and analyzed by electromobility shift assays. The positive control *Mbp* QSBE fragment does interact with QK.
Found at: doi:10.1371/journal.pgen.1001269.s002 (0.82 MB TIF)

Figure S3 QK co-precipitates with *Hnrnpa1* mRNA but not other splicing factors. Formaldehyde crosslinked mouse brain lysate was immunoprecipitated with QK or control His6G antibodies. Co-precipitated RNA was purified and specific RNAs were amplified by RT-PCR followed by separation on an agarose gel. Lanes are as indicated. Note that the *Sfrs5* and *Hnrnpa1* gel images are the same as those presented in Figure 2.
Found at: doi:10.1371/journal.pgen.1001269.s003 (0.24 MB TIF)

Figure S4 QK but not SFRS5 or hnRNP C regulates *Mag* exon 12 inclusion. The isoform ration of *Mag* was assessed as in Figure 5. Transfection with two different *Sfrs5*-targeted siRNAs or two different *Hnrnpc*-targeted siRNAs does not appreciably alter *Mag* isoform ratio relative to control siRNA or a GFP transfection control. In contrast, transfection of a *Qk* targeting siRNA increases *Mag* exon 12 inclusion by two-fold.
Found at: doi:10.1371/journal.pgen.1001269.s004 (0.90 MB TIF)

Figure S5 Correlation coefficient as a function of false discovery rate. Microarray probeset expression values were analyzed as described in the text, for four different False Discovery Rates. Briefly, probesets with changes in expression in both of the *Qk* knockdown groups were selected at the desired FDR. Expression values for the three biological replicates were averaged and the difference from the control CG-4 value was calculated. Correlations between the changes in expression for the indicated groups were calculated using Partek GS Software.
Found at: doi:10.1371/journal.pgen.1001269.s005 (0.34 MB TIF)

Figure S6 Correlation between *Hnrnpa1* knockdown and *Qk* knockdown samples at the transcript level. QK-dependent transcript expression changes are correlated with transcript expression changes caused by hnRNP A1 depletion. Transcripts with expression changes in response to *Qk* knockdown were identified using a two sample t-test, comparing the knockdown groups to the control groups. The mean of each group was determined and the difference from the CG-4 cell line was calculated. Values were clustered as described for Figure 7 for probesets.
Found at: doi:10.1371/journal.pgen.1001269.s006 (0.62 MB TIF)

Table S1 Transcripts significantly changed in response to QK knockdown in CG-4 oligodendrocyte precursor cells.
Found at: doi:10.1371/journal.pgen.1001269.s007 (0.05 MB XLS)

Table S2 Enriched 5mers in alternatively spliced exons.
Found at: doi:10.1371/journal.pgen.1001269.s008 (0.11 MB XLS)

Table S3 Transcripts found to decrease upon QK depletion and containing a QSBE within their 3′ UTR.
Found at: doi:10.1371/journal.pgen.1001269.s009 (0.04 MB XLS)

Table S4 Genes implicated in SCZ that change upon QK depletion.
Found at: doi:10.1371/journal.pgen.1001269.s010 (0.03 MB XLS)

Acknowledgments

This work is dedicated to the memory of Lisa M. McCoig. The authors thank Alison McInnes for helpful discussions, Lynne Hudson for the CG4 and B104 cell lines, Nang Maung and Bill Flaherty for technical assistance, Phyllis Spatrick and the UMass Genomics Core Facility for microarray processing, and Phil Zamore and Reid Gilmore for critical comments on the manuscript.

Author Contributions

Conceived and designed the experiments: NRZ SPR. Performed the experiments: NRZ CCC LMM. Analyzed the data: NRZ CCC BMF SPR. Contributed reagents/materials/analysis tools: NRZ CCC BMF LMM. Wrote the paper: NRZ SPR.

References

1. Lappe-Siefke C, Goebbels S, Gravel M, Nicksch E, Lee J, et al. (2003) Disruption of Cnp1 uncouples oligodendroglial functions in axonal support and myelination. Nat Genet 33: 366–374.
2. Griffiths I, Klugmann M, Anderson T, Yool D, Thomson C, et al. (1998) Axonal swellings and degeneration in mice lacking the major proteolipid of myelin. Science 280: 1610–1613.
3. Li C, Tropak MB, Gerlai R, Clapoff S, Abramow-Newerly W, et al. (1994) Myelination in the absence of myelin-associated glycoprotein. Nature 369: 747–750.
4. Vernet C, Artzt K (1997) STAR, a gene family involved in signal transduction and activation of RNA. Trends Genet 13: 479–484.
5. Sidman RL, Dickie MM, Appel SH (1964) Mutant Mice (Quaking and Jimpy) with Deficient Myelination in the Central Nervous System. Science 144: 309–311.
6. Ebersole T, Rho O, Artzt K (1992) The proximal end of mouse chromosome 17: new molecular markers identify a deletion associated with quakingviable. Genetics 131: 183–190.
7. Hardy RJ, Loushin CL, Friedrich VL, Jr., Chen Q, Ebersole TA, et al. (1996) Neural cell type-specific expression of QKI proteins is altered in quakingviable mutant mice. J Neurosci 16: 7941–7949.
8. Zhao L, Tian D, Xia M, Macklin WB, Feng Y (2006) Rescuing qkV dysmyelination by a single isoform of the selective RNA-binding protein QKI. J Neurosci 26: 11278–11286.
9. Noveroske JK, Hardy R, Dapper JD, Vogel H, Justice MJ (2005) A new ENU-induced allele of mouse quaking causes severe CNS dysmyelination. Mamm Genome 16: 672–682.
10. Li Z, Zhang Y, Li D, Feng Y (2000) Destabilization and mislocalization of myelin basic protein mRNAs in quaking dysmyelination lacking the QKI RNA-binding proteins. J Neurosci 20: 4944–4953.
11. Zhao L, Ku L, Chen Y, Xia M, LoPresti P, et al. (2006) QKI binds MAP1B mRNA and enhances MAP1B expression during oligodendrocyte development. Mol Biol Cell 17: 4179–4186.
12. Larocque D, Galarneau A, Liu HN, Scott M, Almazan G, et al. (2005) Protection of p27(Kip1) mRNA by quaking RNA binding proteins promotes oligodendrocyte differentiation. Nat Neurosci 8: 27–33.
13. Larocque D, Pilotte J, Chen T, Cloutier F, Massie B, et al. (2002) Nuclear retention of MBP mRNAs in the quaking viable mice. Neuron 36: 815–829.
14. Wu JI, Reed RB, Grabowski PJ, Artzt K (2002) Function of quaking in myelination: regulation of alternative splicing. Proc Natl Acad Sci U S A 99: 4233–4238.
15. Aberg K, Saetre P, Lindholm E, Ekholm B, Pettersson U, et al. (2006) Human QKI, a new candidate gene for schizophrenia involved in myelination. Am J Med Genet B Neuropsychiatr Genet 141: 84–90.
16. Aberg K, Saetre P, Jareborg N, Jazin E (2006) Human QKI, a potential regulator of mRNA expression of human oligodendrocyte-related genes involved in schizophrenia. Proc Natl Acad Sci U S A 103: 7482–7487.
17. McCullumsmith RE, Gupta D, Beneyto M, Kreger E, Haroutunian V, et al. (2007) Expression of transcripts for myelination-related genes in the anterior cingulate cortex in schizophrenia. Schizophr Res 90: 15–27.
18. Haroutunian V, Katsel P, Dracheva S, Davis KL (2006) The human homolog of the QKI gene affected in the severe dysmyelination ''quaking'' mouse phenotype: downregulated in multiple brain regions in schizophrenia. Am J Psychiatry 163: 1834–1837.
19. Dracheva S, Elhakem SL, Marcus SM, Siever LJ, McGurk SR, et al. (2003) RNA editing and alternative splicing of human serotonin 2C receptor in schizophrenia. J Neurochem 87: 1402–1412.
20. Dracheva S, Davis KL, Chin B, Woo DA, Schmeidler J, et al. (2006) Myelin-associated mRNA and protein expression deficits in the anterior cingulate cortex and hippocampus in elderly schizophrenia patients. Neurobiol Dis 21: 531–540.
21. Law AJ, Kleinman JE, Weinberger DR, Weickert CS (2007) Disease-associated intronic variants in the ErbB4 gene are related to altered ErbB4 splice-variant expression in the brain in schizophrenia. Hum Mol Genet 16: 129–141.
22. Schmauss C (1996) Enhanced cleavage of an atypical intron of dopamine D3-receptor pre-mRNA in chronic schizophrenia. J Neurosci 16: 7902–7909.
23. Klempan TA, Ernst C, Deleva V, Labonte B, Turecki G (2009) Characterization of QKI gene expression, genetics, and epigenetics in suicide victims with major depressive disorder. Biol Psychiatry 66: 824–831.
24. Backx L, Fryns JP, Marcelis C, Devriendt K, Vermeesch J, et al. (2010) Haploinsufficiency of the gene Quaking (QKI) is associated with the 6q terminal deletion syndrome. Am J Med Genet A 152A: 319–326.
25. Ryder SP, Williamson JR (2004) Specificity of the STAR/GSG domain protein Qk1: implications for the regulation of myelination. Rna 10: 1449–1458.
26. Galarneau A, Richard S (2005) Target RNA motif and target mRNAs of the Quaking STAR protein. Nat Struct Mol Biol 12: 691–698.
27. Hafner M, Landthaler M, Burger L, Khorshid M, Hausser J, et al. (2010) Transcriptome-wide identification of RNA-binding protein and microRNA target sites by PAR-CLIP. Cell 141: 129–141.
28. Zearfoss NR, Farley BM, Ryder SP (2008) Post-transcriptional regulation of myelin formation. Biochim Biophys Acta 1779: 486–494.
29. Louis JC, Magal E, Muir D, Manthorpe M, Varon S (1992) CG-4, a new bipotential glial cell line from rat brain, is capable of differentiating in vitro into either mature oligodendrocytes or type-2 astrocytes. J Neurosci Res 31: 193–204.
30. Ebersole TA, Chen Q, Justice MJ, Artzt K (1996) The quaking gene product necessary in embryogenesis and myelination combines features of RNA binding and signal transduction proteins. Nat Genet 12: 260–265.
31. Li Z, Takakura N, Oike Y, Imanaka T, Araki K, et al. (2003) Defective smooth muscle development in qkI-deficient mice. Dev Growth Differ 45: 449–462.
32. Vasudevan S, Steitz JA (2007) AU-rich-element-mediated upregulation of translation by FXR1 and Argonaute 2. Cell 128: 1105–1118.
33. Wang E, Dimova N, Cambi F (2007) PLP/DM20 ratio is regulated by hnRNPH and F and a novel G-rich enhancer in oligodendrocytes. Nucleic Acids Res 35: 4164–4178.
34. Wang E, Huang Z, Hobson GM, Dimova N, Sperle K, et al. (2006) PLP1 alternative splicing in differentiating oligodendrocytes: characterization of an exonic splicing enhancer. J Cell Biochem 97: 999–1016.
35. Mili S, Steitz JA (2004) Evidence for reassociation of RNA-binding proteins after cell lysis: implications for the interpretation of immunoprecipitation analyses. Rna 10: 1692–1694.
36. Hutchison S, LeBel C, Blanchette M, Chabot B (2002) Distinct sets of adjacent heterogeneous nuclear ribonucleoprotein (hnRNP) A1/A2 binding sites control 5′ splice site selection in the hnRNP A1 mRNA precursor. J Biol Chem 277: 29745–29752.
37. Aguirre A, Dupree JL, Mangin JM, Gallo V (2007) A functional role for EGFR signaling in myelination and remyelination. Nat Neurosci 10: 990–1002.
38. Cui QL, Fogle E, Almazan G (2006) Muscarinic acetylcholine receptors mediate oligodendrocyte progenitor survival through Src-like tyrosine kinases and PI3K/Akt pathways. Neurochem Int 48: 383–393.
39. Gordon D, Kidd GJ, Smith R (2008) Antisense suppression of tau in cultured rat oligodendrocytes inhibits process formation. J Neurosci Res 86: 2591–2601.
40. Mayeda A, Krainer AR (1992) Regulation of alternative pre-mRNA splicing by hnRNP A1 and splicing factor SF2. Cell 68: 365–375.
41. Caceres JF, Stamm S, Helfman DM, Krainer AR (1994) Regulation of alternative splicing in vivo by overexpression of antagonistic splicing factors. Science 265: 1706–1709.
42. Yang X, Bani MR, Lu SJ, Rowan S, Ben-David Y, et al. (1994) The A1 and A1B proteins of heterogeneous nuclear ribonucleoparticles modulate 5′ splice site selection in vivo. Proc Natl Acad Sci U S A 91: 6924–6928.
43. Burd CG, Dreyfuss G (1994) RNA binding specificity of hnRNP A1: significance of hnRNP A1 high-affinity binding sites in pre-mRNA splicing. Embo J 13: 1197–1204.
44. Han K, Yeo G, An P, Burge CB, Grabowski PJ (2005) A combinatorial code for splicing silencing: UAGG and GGGG motifs. PLoS Biol 3: e158. doi:10.1371/journal.pbio.0030158.
45. Emig D, Salomonis N, Baumbach J, Lengauer T, Conklin BR, et al. (2010) AltAnalyze and DomainGraph: analyzing and visualizing exon expression data. Nucleic Acids Res 38 Suppl: W755–762.
46. Wang Z, Rolish ME, Yeo G, Tung V, Mawson M, et al. (2004) Systematic identification and analysis of exonic splicing silencers. Cell 119: 831–845.
47. Zhang Y, Lu Z, Ku L, Chen Y, Wang H, et al. (2003) Tyrosine phosphorylation of QKI mediates developmental signals to regulate mRNA metabolism. Embo J 22: 1801–1810.
48. Umemori H, Kadowaki Y, Hirosawa K, Yoshida Y, Hironaka K, et al. (1999) Stimulation of myelin basic protein gene transcription by Fyn tyrosine kinase for myelination. J Neurosci 19: 1393–1397.
49. Zhang QS, Manche L, Xu RM, Krainer AR (2006) hnRNP A1 associates with telomere ends and stimulates telomerase activity. Rna 12: 1116–1128.
50. Guil S, Caceres JF (2007) The multifunctional RNA-binding protein hnRNP A1 is required for processing fo miR-18a. Nature Structural and Molecular Biology 14: 591–596.
51. Michlewski G, Guil S, Semple CA, Caceres JF (2008) Posttranscriptional regulation of miRNAs harboring conserved terminal loops. Mol Cell 32: 383–393.
52. Dsouza M, Larsen N, Overbeek R (1997) Searching for patterns in genomic data. Trends Genet 13: 497–498.
53. Ule J, Jensen KB, Ruggiu M, Mele A, Ule A, et al. (2003) CLIP identifies Nova-regulated RNA networks in the brain. Science 302: 1212–1215.
54. Ule J, Jensen K, Mele A, Darnell RB (2005) CLIP: a method for identifying protein-RNA interaction sites in living cells. Methods 37: 376–386.
55. Licatalosi DD, Mele A, Fak JJ, Ule J, Kayikci M, et al. (2008) HITS-CLIP yields genome-wide insights into brain alternative RNA processing. Nature 456: 464–469.
56. Jensen KB, Darnell RB (2008) CLIP: crosslinking and immunoprecipitation of in vivo RNA targets of RNA-binding proteins. Methods Mol Biol 488: 85–98.
57. Allen NC, Bagade S, McQueen MB, Ioannidis JP, Kavvoura FK, et al. (2008) Systematic meta-analyses and field synopsis of genetic association studies in schizophrenia: the SzGene database. Nat Genet 40: 827–834.
58. Atz ME, Rollins B, Vawter MP (2007) NCAM1 association study of bipolar disorder and schizophrenia: polymorphisms and alternatively spliced isoforms lead to similarities and differences. Psychiatr Genet 17: 55–67.
59. Inoue K, Osaka H, Sugiyama N, Kawanishi C, Onishi H, et al. (1996) A duplicated PLP gene causing Pelizaeus-Merzbacher disease detected by comparative multiplex PCR. Am J Hum Genet 59: 32–39.

60. Stefansson H, Rujescu D, Cichon S, Pietilainen OP, Ingason A, et al. (2008) Large recurrent microdeletions associated with schizophrenia. Nature 455: 232–236.
61. McCarthy SE, Makarov V, Kirov G, Addington AM, McClellan J, et al. (2009) Microduplications of 16p11.2 are associated with schizophrenia. Nat Genet 41: 1223–1227.
62. Zhang F, Seeman P, Liu P, Weterman MA, Gonzaga-Jauregui C, et al. (2010) Mechanisms for nonrecurrent genomic rearrangements associated with CMT1A or HNPP: rare CNVs as a cause for missing heritability. Am J Hum Genet 86: 892–903.
63. Shaner NC, Campbell RE, Steinbach PA, Giepmans BN, Palmer AE, et al. (2004) Improved monomeric red, orange and yellow fluorescent proteins derived from Discosoma sp. red fluorescent protein. Nat Biotechnol 22: 1567–1572.
64. Pagano JM, Farley BM, McCoig LM, Ryder SP (2007) Molecular basis of RNA recognition by the embryonic polarity determinant MEX-5. J Biol Chem 282: 8883–8894.
65. Tenenbaum SA, Lager PJ, Carson CC, Keene JD (2002) Ribonomics: identifying mRNA subsets in mRNP complexes using antibodies to RNA-binding proteins and genomic arrays. Methods 26: 191–198.
66. Chen-Plotkin AS, Sadri-Vakili G, Yohrling GJ, Braveman MW, Benn CL, et al. (2006) Decreased association of the transcription factor Sp1 with genes downregulated in Huntington's disease. Neurobiol Dis 22: 233–241.
67. Rutledge RG (2004) Sigmoidal curve-fitting redefines quantitative real-time PCR with the prospective of developing automated high-throughput applications. Nucleic Acids Res 32: e178.